

## Low Machining Parameters Produce High Cutting Performance when Machining AISI 1045 at Dry Cutting Conditions Using a CNC Lathe Machine

Iqmal Farhan Rashidi<sup>1</sup>, Norfauzi Tamin<sup>1,\*</sup>, Ridhwan Rani<sup>1</sup>, Umar Al Amani Azlan<sup>2</sup>, Norfariza Ab Wahab<sup>2</sup>, Anwar Ismail<sup>3</sup>, & Agung Setyo Darmawan<sup>4</sup>

<sup>1</sup>Faculty of Technical and Vocational Education, Universiti Tun Hussien Onn Malaysia, Parit Raja, Batu Pahat 86400, Johor, Malaysia

<sup>2</sup>Faculty of Engineering Technology and Manufacturing Industry, Universiti Teknikal Malaysia Melaka, Air Keroh, Melaka 75400, Malaysia.

<sup>3</sup>Pico Play Sdn. Bhd. Lot 5223, Jalan Jeram Batu 26, Pekan Nanas 81500, Johor, Malaysia

<sup>4</sup>Universitas Muhammadiyah Surakarta, Jalan A. Yani, Pabelan, Kartasura, Sukoharjo, Jawa Tengah 57169, Indonesia

\*Corresponding author: norfauzi@uthm.edu.my

### Abstract

AISI 1045 medium-carbon steel is widely used for machining because of its excellent machinability. It balances strength and workability in various manufacturing applications, including machinery parts, gears, mold pins, automotive parts, crankshafts, bolts, and studs. The most significant disadvantage of AISI 1045 machining is that if the cutting parameters are not managed appropriately, it can affect the efficiency of the machining process, which involves tool life and product surface finish at dry cutting conditions. This study aims to determine suitable cutting parameters for AISI 1045, identify the optimum minimum tool wear (VB), and assess surface roughness (Ra). This study used various machining parameters at a cutting speed (Vc) of 35–53 m/min, feed rate (fr) of 0.15, and 0.5 mm/rev at a 1 mm constant depth of cut (DOC). The results showed that a Vc of 35 m/min and a fr of 0.15 mm/rev obtained the lowest average VB of 0.07 mm and Ra of 3.8  $\mu\text{m}$ . This study found that low machining parameters produce high dry-cutting performance. This study provides guidelines for machinists to use appropriate cutting parameters when machining AISI 1045 under dry-cutting conditions at short machining times. In addition, it promotes sustainable machining and prevents air pollution from using coolants (chemical reactions).

**Keywords:** AISI 1045; CNC Lathe; cutting speed; dry cutting; feed rate.

## Introduction

Machining is a manufacturing process that removes material from a workpiece to shape it into the desired form. Machining involves various techniques, such as drilling, milling, grinding, and turning (Ji & Wang, 2019). They are crucial in producing precision parts used in automotive, aerospace, and electronics (Budiman & Mohruni, 2020; Yang & Ming, 2025). Unsuitable parameters can result in poor surface finish, dimensional inaccuracies, VB, and potential damage to the workpiece or the CNC machine. Matching the correct parameters, such as Vc, fr, DOC, and tool selection, to the specific material and geometry of the workpiece is crucial for achieving optimal machining results (Jiang et al., 2020). Besides, if the machining parameters, such as Vc and fr, do not match the workpiece properties and requirements, it can result in various machining issues, such as short tool life and high Ra (Iqbal et al., 2022). To achieve low VB and a refined surface finish in dry machining processes, the machining parameters must align closely with the intrinsic characteristics and requirements of the workpiece. In this case, AISI 1045 is studied to obtain optimal machining parameters and reveal the wear mechanism effects from dry machining work.

The primary objective of this study is to systematically determine the optimal cutting speed (Vc) and feed rate (fr) parameters for the dry machining of AISI 1045 steel using a Computer Numerical Control (CNC) lathe to enhance machining efficiency in terms of surface finish and tool life. The research was done by measuring VB and Ra and

observing the carbide-cutting mechanism, aiming to get the lowest result for both measurements. Finally, the most suitable parameter was acquired, as shown in Figure 1, a methodology flowchart.

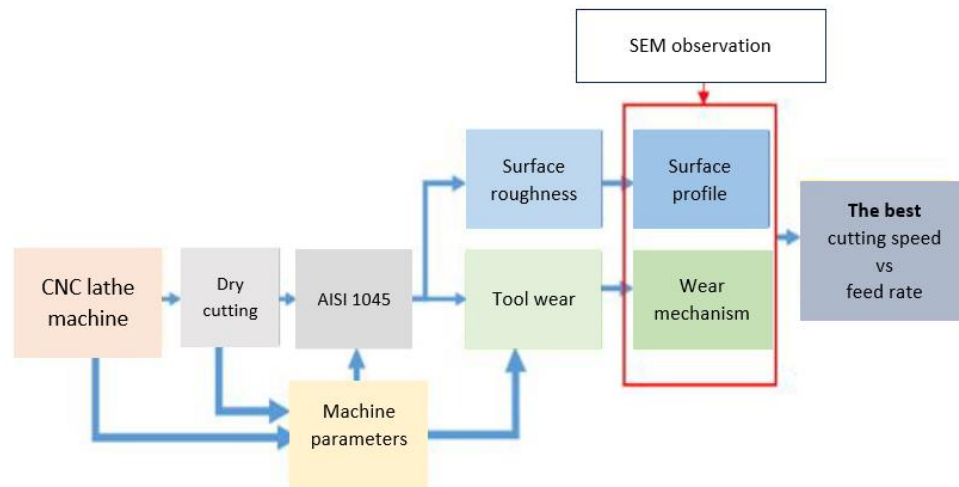


**Figure 1** The flowchart of the methodology.

Unlike other studies, this study was conducted using a CNC lathe machine without any type/method of coolant, such as air spray, minimum quantity lubricator (MQL), or drops of liquid vegetable oil. A significant research gap identified in previous studies is the lack of comprehensive investigations specifically focused on the simultaneous optimisation of cutting speed ( $V_c$ ) and feed rate ( $f_r$ ) for dry machining of AISI 1045 steel using CNC lathes. Existing literature addresses individual cutting parameters or employs different machining conditions, such as cooling strategies, without adequately exploring their combined effects on machining performance metrics under dry cutting. Exposure to the effects on tool wear (VB) and surface roughness (Ra) while observing wear mechanisms and surface integrity has also yet to be explored. The study used a lathe CNC machine due to its significantly advanced machining capabilities, enabling automated and highly precise control over the machining process. CNC lathes provide automated and accurate machining process control (Hatta et al., 2019; Azhar et al., 2020). Lathe machining refers to using a lathe machine to shape and cut materials. According to Faiz et al. (2019), selecting appropriate parameters is crucial for achieving efficient and precise results in lathe machining.  $V_c$ , the velocity at which the workpiece rotates should align with the material properties. Carbon steel commonly uses a  $V_c$  range of 25 to 40 m/min. The feed rate ( $f_r$ ) to determine the tool's advancement per revolution varies based on material and surface finish preferences, with a typical range of 0.1 to 0.5 mm/rev (Jiang et al., 2018). AISI 1045 involves explicitly working with a type of steel known as AISI 1045, and it is commonly used for various applications due to its good machinability, weldability, and moderate strength (Budiman & Mohrni, 2020; Jiang et al., 2020; Iqbal et al., 2022). AISI 1045 finds widespread use in manufacturing due to its favourable mechanical properties and machinability. It is prominently employed for fabricating shafts, gears, and rotating components, requiring a balance of strength and precision (Hatta et al., 2019).

## Materials and Methods

This investigation aimed to evaluate the effectiveness of carbide-cutting tools under dry-cutting conditions while analysing the resultant effects on surface integrity and VB across a range of  $V_c$  and  $f_r$ . The AISI 1045 was chosen for its applicability in manufacturing components such as mould pins and automotive parts. Table 1 provides a comprehensive breakdown of AISI 1045 characteristics.

**Table 1** AISI 1045 chemical composition (Abbas et al., 2019)

Chemical (%)							
G	Simax	Smax	Pmax	Mn	Crmax	CUmax	Nimax
0.42–0.5	0.4	0.045	0.04	0.5–0.8	0.3	0.3	0.4
Mechanical characteristics							
Re [MPa]	Rm [MPa]		As (%)		HB		
305	580		16		250		

The AISI 1045 for machine work is 250 mm long and 70 mm in diameter. It is machined using a CNMG 120408 type and LAMINA brand carbide-coated cutting tool that is securely clamped in a tool holder, as shown in Figure 2.

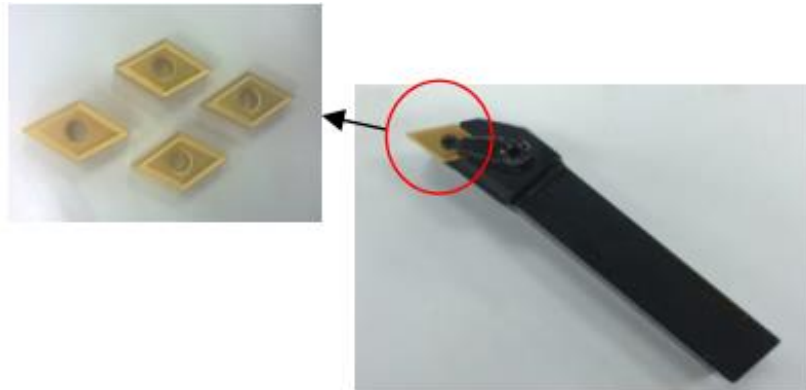


**Figure 2** Cutting tool attached to the tool holder.

This study investigates the influence of  $V_c$ ,  $f_r$ , and constant DOC on VB and Ra in machining operations. The AISI 1045 was machined using a carbide-coated cutting tool on a CNC turning machine. The dry-cutting condition parameters were selected based on previous studies that performed wet-cutting conditions on AISI 1045 (Jiang et al., 2019), as shown in Table 2.

**Table 2** Cutting parameter

$V_c$ (m/min)	$f_r$ (mm/rev)	Constant DOC (mm)
35	0.15	1
41	0.15	
47	0.15	
53	0.15	
35	0.50	
41	0.50	
47	0.50	
53	0.50	

VB was measured according to ISO 3685 standards utilising the optical microscope with Dino-lite brand, as shown in Figure 3(a). The measurement of average VB, mainly flank wear, is critical to evaluating cutting tool performance in machining processes, as outlined in ISO 3685 (Tamin et al., 2017; Bakar et al., 2018). According to this standard, the width of the flank wear land (VB) is the parameter for assessing tool life. A uniform wear profile allows continued tool use unless the average VB exceeds 0.3 mm. Figure 3(b) shows a surface roughness tester with the Leeb452 brand for Ra measurement. Ra has been observed morphologically through scanning electron microscopy (SEM) to investigate the surface characteristics after machining. The results, discussed in the subsequent sections, provide insights into the optimal machining conditions for minimising VB and Ra, contributing to the understanding of precision machining processes on AISI 1045.

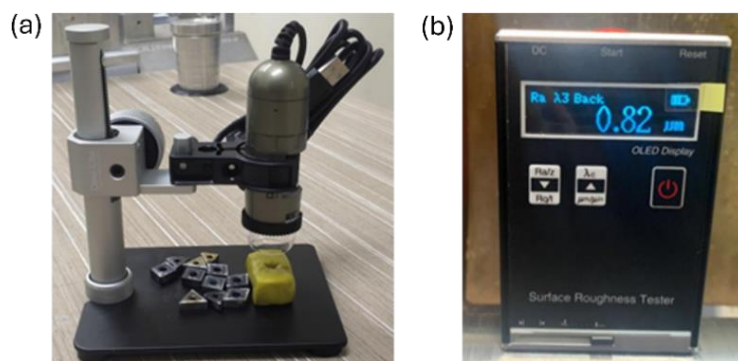


**Figure 3** Measurement equipment of (a) optical microscope and (b) surface roughness tester.

## Result

Figure 4 shows a  $f_r$  of 0.15 mm/rev, a tremendous increase in VB observed values with increasing  $V_c$  from 35 to 53 m/min, which is equivalent to a 100% increase. However, it is below 0.3 mm (as specified in the ISO 3685 standard). The line graph reinforces this correlation, highlighting a direct and positive relationship between VB and  $V_c$  under a 0.15 mm/rev  $f_r$ . Meanwhile, a 0.50 mm/rev  $f_r$  recorded a 125% increase in VB values (from 0.08 mm to 0.18 mm), corresponding to a rise in  $V_c$  from 35 to 53 m/min. As a result, rising temperatures are the leading cause of increasing  $V_c$  and, consequently, increasing VB. This scenario arises because of the elevated friction, leading to a more pronounced deterioration of the tool.

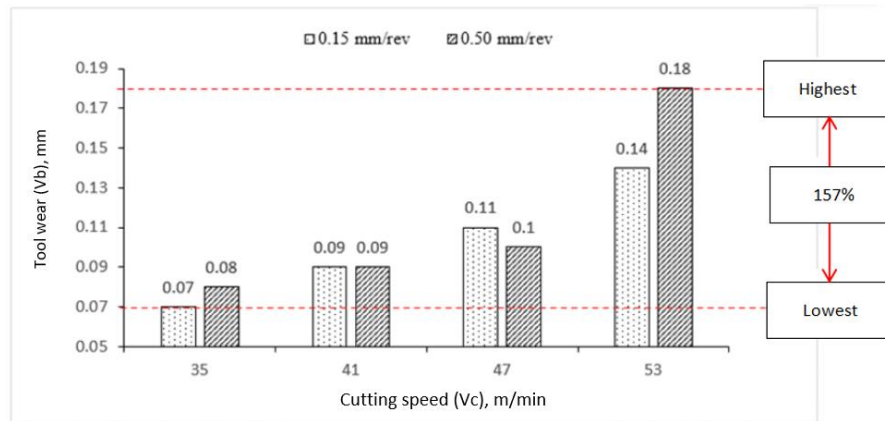


Figure 4 VB comparison.

Nevertheless, the 0.15 mm/rev  $f_r$  dominates the lowest VB at all  $V_c$ . The influence of  $f_r$  on achieving long tool life has been emphasised in various studies, highlighting its importance in minimising wear and enhancing machining performance. The  $f_r$  influence of VB in machining processes has been extensively investigated. Salur et al. (2021) highlighted that a higher  $f_r$  increases VB due to the increasing material removal rate. Similarly, Kuntoğlu (2021) found that VB increased with increasing  $f_r$ . This observation underscores the intricate interplay between  $f_r$  and  $V_c$  in influencing the VB. These findings underscore the critical importance of meticulous parameter adjustments for balancing  $V_c$ ,  $f_r$ , and VB in optimising AISI 1045 machining processes.

## Wear Mechanism

Figure 5(a) shows crater wear, which shows the gradual material loss at the contact interface, representing both flank and crater wear at 0.15 mm/rev  $f_r$ . In the initial stages of contact, the cutting tool shears the metals and shapes the surface under the tool nose radius. As machining progresses, the sliding and friction from the cutting tool against the AISI 1045 generates elevated temperatures, causing a gradual material loss in certain sections of the cutting tool and resulting in an uneven nose radius shape of the cutting edge. Further machining induces minor vibrations and fractures at the cutting tool's edge. While Figure 5(b) shows severe cutting-edge conditions when employing a 0.50 mm/rev  $f_r$ . Observable in the figure are signs of chipping along the cutting edge. Flank wear can occur at both cutting speeds; however, the type of mechanism is different due to excessive wear.

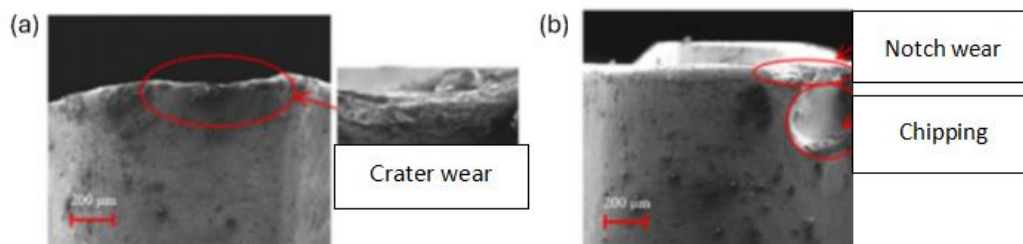


Figure 5 Wear formation at 53 m/min cutting speed.

Figure 6 shows the VB mechanism from a top view at a  $V_c$  of 53 m/min. Figure 6(a) at an  $f_r$  of 0.15 mm/rev shows the crater wear mechanism. When  $f_r$  increases to 0.50 mm/rev, flaking appears on the rake face, as shown in Figure 6(b). Flaking can

potentially exacerbate cutting tool damage by promoting movement in the grain structure and creating openings for chip or debris attachment along the cutting edge. Ultimately, this process can lead to significant damage and occur of built-up edge (BUE). The formation of BUE is influenced by the stick-slip phenomenon at the interface between the chip and the cutting tool, which is linked to the self-organised critical process (SOC) (Rabinovich et al., 2022). Indirect adhesion wear (BUL and BUE) has been identified as the leading cause, and this wear mechanism is due to an inappropriate feed rate (Javier et al, 2021).

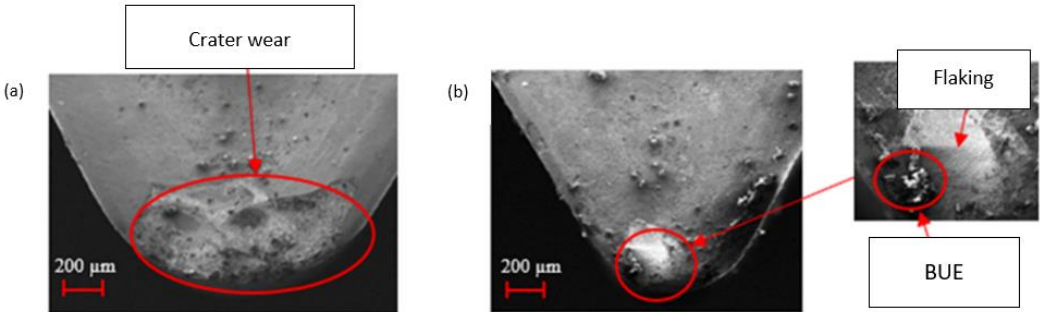


Figure 6 Top view formation.

Figure 6 Top view formation.

Surface Roughness

Figure 7 shows a comparison of Ra between different fr and various Vc. Ra was observed with increasing Vc at both fr of 0.15 mm/rev and 0.50 mm/rev. However, at a fr of 0.15 mm/rev, the Ra decreased by up to 31% when the Vc was increased to 53 m/min. The variability in Ra profiles can be attributed to the impact of cutting parameters, including fr and Vc. Studies by Zhou et al. (2019) have shown that improper selection or control of cutting parameters can lead to non-uniform Ra profiles. Variations in fr and Vc can result in inconsistent material removal and chip formation, leading to an uneven surface finish. The consistent increase in Ra shown at a fr of 0.50 mm/rev is due to the Vc and fr used being parallel. The elevated fr and Vc correlate with increased Ra levels, and this finding is parallel to those of Suresh and Poongodi (2018), who stated that the Ra increases with the fr increase. The study demonstrated that higher fr resulted in elevated Ra due to increased tool-chip contact and the generation of a more prominent BUE on the cutting tool. The higher fr led to a more pronounced transverse movement of the tool nose radius, resulting in more significant feed marks, an increased peak-to-peak value gap, and elevated Ra. It is similar to the findings from Martins et al. (2023) found that the Ra increases with rising Vc.

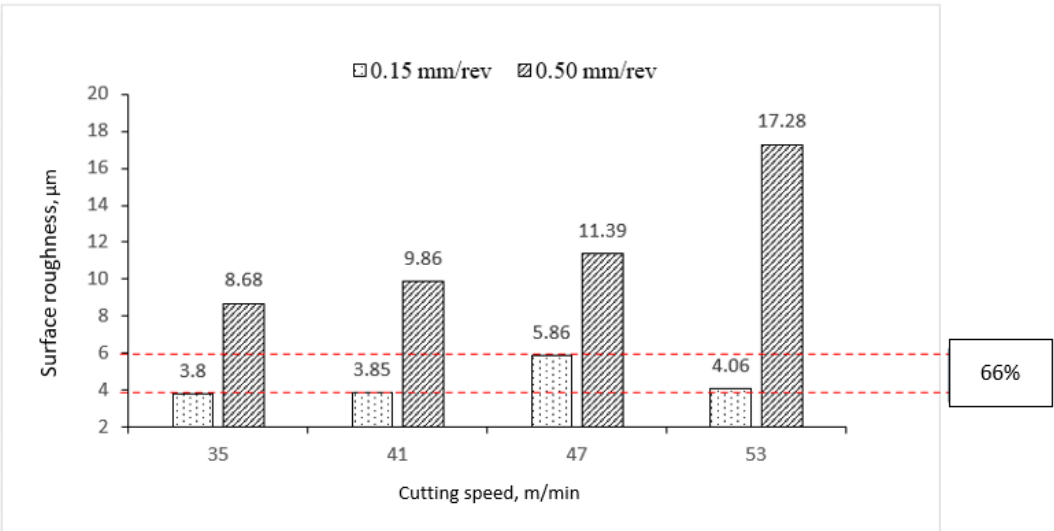
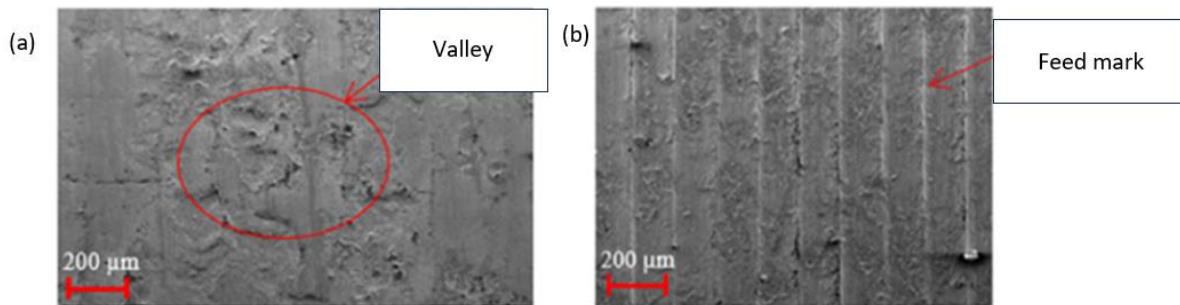


Figure 7 Cutting speed vs Ra.

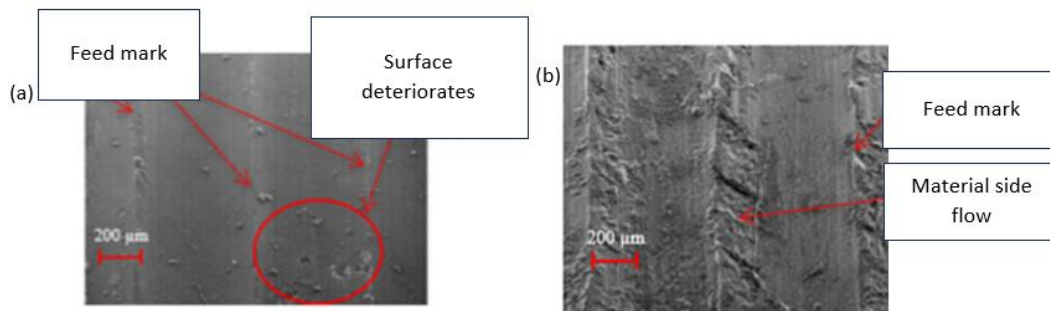


Figure 8(a) shows the surface characteristics of AISI 1045 when using a 47 m/min Vc at 0.15 mm/rev fr. The character shows that certain parts of the surface profile exhibit the formation of valleys with significant smearing, which creates a uniform peak. Nevertheless, there are no discernible feed marks, and a lack of side-flow material is present, contributing indirectly to a smooth and shiny surface on AISI 1045. Observations indicate that valleys do not hinder smooth and shiny surfaces. However, as the Vc increases to 53 m/min, as shown in Figure 8(b), feed marks become visibly prominent in the surface profile throughout the machining process, aligning with higher Ra.



**Figure 8** The appearance of feed marks on the surface.

Figure 9 shows the surface profile during the machining of AISI 1045 under (a) 35 and (b) 53 m/min Vc with a 0.50 mm/rev fr. It was observed that the initial machining stages at 35 m/min Vc, as shown in Figure 9(a), exhibited a remarkably smooth and little feed mark. Compared to 53 m/min Vc, feed marks are formed along AISI 1045 along with the sizeable lateral flow, indirectly affecting the Ra results as shown in Figure 9(b).



**Figure 9** Surface profile at a feed rate of 0.50 mm/rev.

Based on the research findings demonstrating that low machining parameters lead to minimal VB and Ra when machining AISI 1045 under dry-cutting conditions, a promising avenue for future investigation could explore optimising cutting parameters using advanced computational modelling and simulation techniques. This research could delve deeper into understanding the intricate interplay between cutting parameters such as Vc, fr, and DOC, along with their impact on VB and surface quality. Researchers can systematically explore various machining conditions by employing sophisticated modelling approaches to identify optimal parameter combinations that minimise VB while maintaining a superior surface finish. Additionally, integrating experimental validation with computational simulations can enhance the accuracy and reliability of the findings, paving the way for developing more efficient and sustainable machining processes for AISI 1045 and similar materials.

## Discussion

Vc results in different flank wear effects when using different fr, where a higher fr accelerates the wear process and produces various wear mechanisms such as crater wear, flaking, and chipping. Vc and fr affect VB, where high Vc and fr increase friction and stress. The Vc and fr were the two machining parameters with the most significant impact on the VB, while the axial cutting depth had the least (Kaladhar et al., 2012; Afif et al., 2024). When ferrous materials are machined, the cutting temperature rises as the cutting velocity increases, resulting in the cutting tool's softening and causing the cutting tool to experience rapid wear and tear and then fail to function correctly. Additionally, Wei et al. (2021) observed a decrease in tool life as Vc increased. Guo et al. (2017) discovered that the pressures used in cutting

and the resulting machining quality varied with  $V_c$ . Crater wear is recognised as the antecedent to flank wear, as it necessitates edge deterioration before the advancement of plastic deformation onto the tool flank.

Flank and crater wear co-occur in cutting tools due to the complex interactions between the cutting tool and the workpiece. Gurbuz and Gonulacar (2020) attributed flank wear to abrasion between the work surface and the flank face, while crater wear was linked to the exchange of atoms across the tool-chip interface. Further emphasis was placed on the distinct flank and crater wear locations, with the former occurring at the minor cutting-edge flank face and the latter near the significant cutting-edge rake face. According to Abbas et al. (2019),  $V_c$  increases can produce high friction at the contact of the cutting tool and the workpiece, which in turn causes high pressure on the rake face of the cutting tool, resulting in crater and flank wear. In addition, crater wear also occurs due to the contact between the tip of the cutting tool and the chip that rubs against AISI 1045 during machining, generating heat at the point of contact. This repetitive contact at low  $f_r$  intensifies shear friction, leading to increased material loss at the cutting point (Peksen & Kalyon, 2021). Crater wear is identified as a significant wear mode in cutting tools during machining processes. The crater wear is influenced by various factors, such as  $V_c$ ,  $f_r$ , and the workpiece material (Saifuldin et al., 2024). The wear mechanism of crater wear involves a combination of adhesion, abrasion, dissolution, and diffusion, leading to the gradual development of craters (Wei et al., 2021). This wear phenomenon arises from the prolonged interaction between the cutting tool and AISI 1045, producing chips via abrasive sliding against the workpiece material. Subsequently, these chips progressively mass at the cutting tool's edge, inducing friction during machining procedures. This friction results in a substantial increase in temperature at the cutting end, leading to the gradual flaking and plucking of the grain in the carbide-cutting tool (Guo et al., 2017). Flaking may stem from either the abrasive action of a hard-sliding chip or the friction between the chip and the cutting tool's tip. Friction causes temperature distribution at the tool-chip interface and has implications for VB mechanisms, including flaking, and subsequently produces chipping at the tip of the cutting tool. Hence, the elevated temperature resulting from this friction gives rise to a chip that extends onto the rake face, causing abrasive wear. Abrasive wear enlarges the contact area and raises the machining temperature at the cutting tool interface, leading to adhesion on the rake face (Salur et al., 2021). Besides flaking, the phenomenon of chipping wear may result from intense collisions during the initial contact, causing the breakage of small sections.

Furthermore, the absence of cutting fluid or coolant, as well as inappropriate cutting parameters, can contribute to chipping. The significant influence of edge radii on VB indicates that inappropriate cutting conditions and machining parameters can lead to flaking and chipping on the rake face (Azhar et al., 2020). Chipping wear on the cutting tool during dry cutting can be attributed to various factors. For instance, Saifuldin et al. (2024) highlighted that flank wear, chipping, and catastrophic failures result from abrasion and adhesion at the cutting tool face, emphasising the importance of tool selection when machining nickel-based alloys. Additionally, chipping may occur due to gradual material loss, which alters the tool's nose radius. The combination of high  $f_r$  and elevated temperatures may lead to the detachment of small material portions from the cutting tool's edge due to the grain structure moving due to contact and high friction.

The effects of various VB produce different surface profiles, but the most noticeable is the presence of peaks and valleys. The peaks and valleys on the product surface directly influence their smoothness and shininess (Gurbuz & Gonulacar, 2020). Zhou et al. (2019) stated that high-speed machining causes increased  $R_a$  due to the formation of clear material flow, the occurrence of adhesion of metal fragments on the surface, and feed marks along the material. This occurrence may be attributed to the wear and uneven shearing of the cutting tool's end due to repeated machining, leading to an uneven nose radius. This degradation can be attributed to wear on the cutting tool edge, resulting in increased friction during the machining process. Feed marks on workpiece surfaces become more significant with the increase of  $V_c$  and  $f_r$  (Hua & Liu, 2019). This observation found that the elevated  $f_r$  induced a material-pushing effect towards the side, resulting in material displacement from the feed mark's parallel ridge. Consequently, the material grain pulled out during machining, causing scratches on the surface (Norfauzi et al., 2024). These particles overlapped, leading to a significant increase in  $R_a$  and, indirectly, a shortened tool life for the cutting tool. According to Jose et al. (2018), under elevated  $V_c$  and  $f_r$  conditions, frequent reciprocating movements between the cutting tool and the workpiece led to high temperatures attributed to friction and contact. This rise in temperature during machining produces a softening effect on the machined surface. When the cutting tool deviates from the shearing zone, the softened surface undergoes plasticisation towards the feed marks' side, resulting in the appearance of material side flow on the ridge (Sandin et al., 2023). Further, material side flow arises in machining as the sheared workpiece experiences plastic deformation induced by elevated cutting temperatures. Concurrently, the cutting tool displaces the material, resulting in the formation of a

deformed layer. This lateral flow of material presents a heightened susceptibility to fatigue failure, particularly when the workpiece is subjected to rotational applications.

## Conclusion

The investigation focuses on the effects of variations in  $V_c$  and  $f_r$  on  $VB$  and  $R_a$  in dry-cutting conditions on AISI 1045. The overall conclusion from this study was that the lowest measurement results or the most optimal parameters on cutting  $VB$  and  $R_a$  were dominated by the feed rate of 0.15 mm/rev. However, increased  $V_c$  and  $f_r$  led to heightened value  $VB$ , marked by chipping, crater wear, flank wear, and BUE on the carbide-cutting tool. The situation was attributable to intensified forces and initial contact between the cutting tool and AISI 1045. Based on the results, the machining parameters ( $V_c$  and  $f_r$ ) used are below 0.3 mm for average  $VB$ . Referring to the ISO 3685 standard, a uniform wear profile allows continued tool use unless the average  $VB$  exceeds 0.3 mm. Additionally, the increase in  $V_c$  can influence  $R_a$ , with prolonged friction periods causing elevated temperatures due to the absence of cutting fluid, affecting contact points within the cutting zone. Surface profile analysis unveiled feed marks, fluctuations in peak and valley formations, and lateral material flow, with  $R_a$  imperfections contingent on machining parameters and the absence of cutting fluid or coolant. Future recommendations are that there is a critical need to explore a broader range of machining parameters through statistical methods to extend tool life and improve the surface finish, thereby promoting sustainable machining. This is because dry-cutting friction requires a constant parameter between  $V_c$ ,  $f_r$ , and  $DOC$  to obtain a high tool life due to the friction between the cutting tool and the work material.

## Acknowledgments

The authors would like to thank the grant Tier 1 Q919, Universiti Tun Hussien Onn Malaysia, for the research facilities provided during the project.

## Compliance with ethics guidelines

The authors declare they have no conflict of interest or financial conflicts to disclose.

This article contains no studies with human or animal subjects performed by authors.

## References

- Abbas A. T., Al Bahkali, E. A., Alqahtani, S. M., Abdelnasser, E., Naeim, N., & Elkaseer, A. 2021. Fundamental investigation into tool wear and surface quality in high-speed machining of Ti6Al4V alloy. *Materials (Basel)*, 14 (7128), 1–19.
- Abbas, A. T., Benyahia, F., El Rayes, M. M., Pruncu, C., Taha, M. A., & Hegab, H. 2019. Towards optimization of machining performance and sustainability aspects when turning AISI 1045 steel under different cooling and lubrication strategies. *Materials (Basel)*, 12 (3023), 1–17.
- Afif, I. Y., Jamari, J., Saputra, E., Saefudin, S., Subri, M., & Amin, M. 2024. Exploring wear characteristics of AISI 1045 steel under variable disc rotation speeds: a tribological investigation. *Teknik*, 45 (1), 111–116. doi: 10.14710/teknik.v45i1.59720.
- Azhar, A. A., Azlan U. A. A., Bakar, H. A., Tamin, N., Herawan, S. G., & Ahmad, Z. 2020. Friction comparison and wear analysis of ceramic cutting tools made from alumina-zirconia-chromia content. *Journal of Advanced Research in Applied Mechanics*, 112 (1), 175–182.
- Bakar, H., Fahmi, N., Mokhtar, F., Tamin, N., Azlan, U., Adam, A.A., Izamshah, R., & Kasim, S. 2018. Fabrication and Machining Performance of Powder Compacted Alumina-Based Cutting Tool. *MATEC Web Conferences*, 150, 2–6, doi: 10.1051/mateconf/201815004009.
- Budiman, A. Y., & Mohruni, A. S. 2020. A review on thin-walled cryogenic machining on inconel or aerospace materials. *Journal of Mechanical Science and Engineering*, 7 (1), 001–005.
- Faiz, M. M., Hairizal, M., Naim, M. F., Norfauzi, T., Umar, U. A.A., Aziz, A. A., & Noorazizi, S.M. M. 2019. Effect of hydraulic pressure on hardness, density, tool wear and surface roughness in the fabrication of alumina-based cutting tool. *Journal of Advance Manufacturing Technology*, 13 (1), 23–37.
- Guo, X., Zhu, Z., Ekevad, M., Bao, X., & Cao, P. 2017. The cutting performance of Al<sub>2</sub>O<sub>3</sub> and Si<sub>3</sub>N<sub>4</sub> ceramic cutting tools in the milling plywood. *Advances in Applied Ceramics*, 6753 (9), 1–8.



- Gurbuz, H., & Gonulacar, Y. E. 2020. Optimization and evaluation of dry and minimum quantity lubricating methods on machinability of AISI 4140 using Taguchi design and ANOVA. *Proceeding of Mechanical Engineering Science*, 1–17. doi: 10.1177/0954406220939609.
- Hatta, W. N., Jafar, F. A., Nor, F. M., & Noor, A. Z. M. 2019. Machinability performance of CNC turning based on automated coolant supply system. *International Journal of Innovative Technology and Exploring Engineering*, 8 (10), 3953–3957.
- Iqbal, A., Zhao, G., Cheok, Q., He, N., & Nauman, M. M. 2022. Sustainable machining: tool life criterion based on work surface quality. *Processes*, 10 (6), 1087.
- Hua, Y., & Liu, Z. 2019. Effects of Machining Induced Residual Shear and Normal Stresses on Fatigue Life and Stress Intensity Factor of Inconel 718. *Applied Sciences*, 9 (4750), 1–17.
- Javier, F., Vilches, T., Mart, S., Gamboa, C. B., Herrera, M., & Hurtado, L. S. 2021. Influence of tool wear on form deviations in dry machining. *Metals (Basel)*, 11 (958), 1–22.
- Ji, W., & Wang, L. 2019. Industrial robotic machining: a review. *International Journal of Advanced Manufacturing Technology*, 103 (1–4), 1239–1255.
- Jiang, Z., Gao, D., Lu, Y., & Shang, Z. 2020. Optimisation of cutting parameters for minimising carbon emissions and cost in the turning process. *Journal of Mechanical Engineering and Sciences*, pp. 1–13.
- Jose, D. A., Antonio, D. Á., Migu, H., & Cantero, L. 2018. Finishing turning of ni superalloy haynes 282. *Metals (Basel)*, 8 (843), 1–12. doi: 10.3390/met8100843.
- Kaladhar, M. 2020. Optimization of machining parameters when machining beyond recommended cutting speed. *World Journal of Engineering*, 17 (5), 739–749. doi: 10.1108/wje-01-2020-0018.
- Martins, A. M., Oliveira, D. A., Magalhães, F. C., & Abrão, A. M. 2023. Relationship between surface characteristics and the fatigue life of deep rolled AISI 4140 steel. *International Journal of Advanced Manufacturing Technology*, 129 (3–4), 1127–1143.
- Norfauzi, T., Hamid, A., Azlan, U. A. A., & Ali, M. B. 2024. Optimising cutting parameters of aisi h13 to reduce tool wear and surface roughness in the lathe cnc machining process. *Journal of Advanced Manufacturing Technology (JAMT)*, 18 (3), 15–18. doi: 10.1201/9781482278804-7.
- Peksen, H., & Kalyon, A. 2021. Optimization and measurement of flank wear and surface roughness via Taguchi-based grey relational analysis. *Materials Manufacturing Process*, 1–10. doi: 10.1080/10426914.2021.1926497.
- Rabinovich, G. F., Gershman, I. S., Yamamoto, K., & Dosbaeva, J. 2020. Effect of the adaptive response on the wear behavior of PVD and CVD coated cutting tools during machining with built-up edge formation. *Nanomaterials*, 10 (2489), 1–22.
- Saifuldin, M., Mokhtar, M., Yusoff, A. R., & Lubis, M. S. Y. 2024. Effect of machining parameters on micro-burrs formation of aluminium puncher using high-speed machining process. *Journal of Advanced Research in Applied Mechanics*, 1 (1), 47–60.
- Salur, E., Kuntoğlu, M., Aslan, A., and Pimenov, D. Y. 2021. The effects of MQL and dry environments on tool wear, cutting temperature, and power consumption during end milling of AISI 1040 steel. *Metals (Basel)*, 11 (1674), 1–17.
- Sandin, O., Prieto, J. M. R., Hammarberg, S., & Casellas, D. 2023. Numerical modelling of shear cutting using particle methods. *IOP Conference Series: Materials Science and Engineering*, 1284 (1), 012048. doi: 10.1088/1757-899x/1284/1/012048.
- Suresh, P., & Poongodi, T. 2018. Evaluation of surface roughness during turning of Al-SiC and Al-SiC-Gr composites. *Multidiscip. Model. Mater. Struct.*, 14 (5), 874–890.
- Tamin, N. F., Azlan, U. A. A., Remle, N. S., & Osman, M. H. 2017. Study on surface integrity of AISI 1045 carbon steel when machined by carbide cutting tool. *MATEC Web Conferences*, 01075 (97), 2–6. doi: 10.1051/mateconf/20179701075.
- Wei, W., Li, Y., Xu, Y., & Yang, C. 2021. Research on tool wear factors for milling wood-plastic composites based on response surface methodology. *Bioresources*, 16 (2008), 151–162.
- Yang, Q., & Ming, W. 2025. Review: application of green manufacturing processes in precision machining of automotive components. *Green Manufacturing Open*, 3(1), 3-10. doi: 10.20517/gmo.2024.120501.
- Zhou, T., He, L., Wu, J., Du, F., & Zou, Z. 2019. Prediction of surface roughness of 304 stainless steel and multi-objective optimisation of cutting parameters based on GA-GBRT. *Applied Sciences*, 9 (3684), 1–22.